

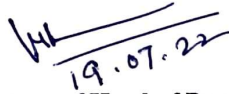
CERTIFICATE

It is certified that the work contained in the thesis titled **“Investigation of Design and Analysis of Partially Dielectric Filled Coaxial Disc Loaded Magnetically Insulated Line Oscillator (MILO)”** by **“Nisheeth Upadhyay”** has been carried out under our supervision and that this work has not been submitted elsewhere for a degree.

It is further certified that the student has fulfilled all the requirements of Comprehensive, Candidacy, and SOTA for the award of Ph. D. Degree.



(Dr. Smrity Dwivedi)
Supervisor
Dept. of Electronics Engineering
IIT (BHU), Varanasi




Signature of Head of Department
"SEAL OF THE DEPARTMENT"

आचार्य व विभागाध्यक्ष/PROFESSOR & HEAD
इलेक्ट्रॉनिकी अभियांत्रिकी विभाग/Department of Electronics Engineering
भारतीय प्रौद्योगिकी संस्थान (का.हि.वि.)/Indian Institute of Technology (IIT)
वाराणसी/Varanasi-221005 (INDIA)

DECLARATION BY THE CANDIDATE


I, Nisheeth Upadhyay, certify that the work embodied in this thesis is my own bonafide work and carried out by me under the supervision of Dr. Smrity Dwivedi from July 2017 to July 2022, at the Department of Electronics Engineering, Indian Institute of Technology (BHU), Varanasi. The matter embodied in this thesis has not been submitted for the award of any other degree/diploma. I declare that I have faithfully acknowledged and given credits to the research workers wherever their works have been cited in my work in this thesis. I further declare that I have not wilfully copied any other's work, paragraphs, text, data, results, *etc.*, reported in journals, books, magazines, reports, dissertations, thesis, *etc.*, or available at websites and have not included them in this thesis and have not cited as my own work.

Date: 19/07/22
Place: IIT, BHU


Signature of the Student
Nisheeth Upadhyay

CERTIFICATE BY THE SUPERVISORS

It is certified that the above statement made by the student is correct to the best of my knowledge.


(Dr. Smrity Dwivedi)
Supervisor
Dept. of Electronics Engineering
IIT (BHU), Varanasi

COPYRIGHT TRANSFER CERTIFICATE

Title of the Thesis: Investigation of Design and Analysis of Partially Dielectric Filled Coaxial Disc Loaded Magnetically Insulated Line Oscillator (MILO)

Name of the Student: Nisheeth Upadhyay

Copyright Transfer

The undersigned hereby assigns to the Indian Institute of Technology (Banaras Hindu University), Varanasi all rights under copyright that may exist in and for the above thesis submitted for the award of the Doctor of Philosophy.

Date: 19/07/22

Place: IIT, BHU



Signature of the Student

Nisheeth Upadhyay

Note: However, the author may reproduce or authorize others to reproduce material extracted verbatim from the thesis or derivative of the thesis for author's personal use provided that the source and the Institute's copyright notice are indicated.

ACKNOWLEDGEMENTS

Foremost, I would like to express my immense gratitude to my supervisor **Dr. Smrity Dwivedi** for their excellent guidance and motivation. The completion of this research work is truly an outcome of their constant untiring support, valuable ideas, and suggestions during my research work. The insightful discussions with them always provided me great enthusiasm. I could not have imagined having better advisors and mentors for my research work.

I wish to extend my sincere gratitude towards my research performance evaluation committee (RPEC) members, **Dr. M. Thottappan** and **Prof. R. Mahanty** for their encouragement and insightful comments. I also thank to all faculty members for their kind cooperation and encouragement during this journey.

My special thanks to Dr. Manpuran Mahto, Dr. Siva Venkateswara Rao V., Dr. Vikram Kumar, Dr. Rajan Agrahari, Dr. A. P. Singh, Dr. Anshu Sharan Singh, Dr. Prabhakar Tripathi, Dr. R. K. Singh, Dr. M. A. Ansari, Dr. Akash, and Dr. Vineet Singh for their valuable assistance from personal to the technical level.

I am very much thankful to many research scholars of the CRMT laboratory for providing a stimulating and friendly environment. My thanks go to, Mr. Sambit, Mr. Dipti, Mr. Nilotpal, Mr. Soumjit, Mr. V. V. Reddy, Mr. V. Veera Babu, Mr. G. Venkatesh, and Mr. S. G. Yadav.

My thanks and sincere appreciations also go to all staff members of the CRMT laboratory, especially to Mr. Rajesh Kr. Rai for their kind co-operation.

I also thank my colleagues, Mr. Amit Sisodia, Mr. Ankit, Mr. Amit Kumar, and Mr. Azhar Khan, for providing a fun-filled environment.

I deeply admire my Brothers, Sisters, and my close friends Mr. Chandramani Yadav and Mr. Srish Upadhyay for their continued support and encouragement. They are the source of strength for me and remain an invaluable asset to me.

I would like to express my special thanks to my wife Er. Ankita and my son Master Anagh for her patience and continued support. She supported me a lot during these times.

Finally, I heartily express sincere thanks to my parents Shri. Ram Prakash Upadhyay and Smt. Geeta. I wish to express indebtedness to them, for their unconditional love,

extreme patience, and constant support over the years. They provide me the strength and confidence to attain this task.

Above all, I bow my head before almighty Lord Vishwanath for providing me the strength and courage in completing my research work.

Date: 19/07/22


(Nisheeth Upadhyay)

*Dedicated
To
My Supervisor
&
My Family*

CONTENTS

<i>List of Figures</i>	xiii-xvi	
<i>List of Tables</i>	xvii	
<i>List of Abbreviations</i>	xviii-xix	
<i>List of Symbols</i>	xx-xxii	
<i>Preface</i>	xxiii-xxiv	
CHAPTER 1	INTRODUCTION AND LITERATURE REVIEW	1-47
1.1.	Introduction	2
1.2.	Origin and Classification of HPM	3
1.3	Overview and Evaluation of Distinct HPM Tubes	5
1.3.1	Relativistic Klystron Amplifier (RKA) and Relativistic Klystron Oscillator (RKO)	8
1.3.2.	Relativistic Backward Wave Oscillator	11
1.3.3.	Virtual Cathode Oscillator (VIRCATOR)	12
1.3.4.	Reltron	13
1.3.5.	Arletron	15
1.3.6.	Relativistic Gyro Devices	16
1.3.7.	Plasma Assisted Slow- Wave Oscillator (PASOTRON)	17
1.3.8	Transit -Time Oscillator (TTO)	18
1.3.9	Split Cavity Oscillator (SCO)	20
1.3.10	Relativistic Magnetron	21
1.4.	Magnetically Insulated Line Oscillator (MILO)	23

1.4.1.	Sub-assemblies Description	25
1.4.2.	Principle of Operation	28
1.5.	Literature Review on MILO	31
1.5.1	MILO Development Time Line	31
1.5.2	Literature Review	34
1.6.	Motivation and Research Objective	42
1.6.1	Motivation	42
1.6.2	Research Objective	43
1.7.	Plane and Scope	45
CHAPTER 2	ELECTROMAGNETIC ANALYSIS OF AN AXIALLY PERIODIC DISK-LOADED SLOW-WAVE STRUCTURE WITH LOW-LOSS DIELECTRIC FILLING BETWEEN DISKS FOR A MAGNETICALLY INSULATED LINE OSCILLATOR	48-74
2.1.	Outline	49
2.2.	Introduction	49
2.3.	Analytical approach	52
2.3.1	EM Field Expression for Region- I (i.e., $r_c < r < r_d$)	54
2.3.2	EM Field Expression for Region- II (i.e., $r_d < r < r_{DI}$)	56
2.3.3	EM Field Expression for Region- III (i.e., $r_{DI} < r < r_w$)	57
2.4	Boundary Conditions	58
2.5	Dispersion Relationship	59
2.5.1	For Region – II and III	59

2.5.2	For Region – I and II	61
2.6	Interaction Impedance	63
2.7	Results and Discussion	67
2.7.1	Parametric Study on Dispersion Relationship	71
2.7.2	Parametric Study on Interaction Impedance	73
2.8	Conclusion	74

**CHAPTER 3 Beam-Wave interaction analysis of an axially periodic
Disk-Loaded slow-wave structure with low-loss**

	Dielectric filling between disks for a MILO	75-97
3.1.	Outline	76
3.2.	Introduction	76
3.3.	Analytical approach	79
3.3.1.	EM Field Expression for Region- I (i.e., $r_c < r < r_e$)	81
3.3.2.	EM Field Expression for Region- II (i.e., $r_e < r < r_d$)	84
3.3.3.	EM Field Expression for Region- III (i.e., $r_d < r < r_{DI}$)	85
3.3.4.	EM Field Expression for Region- IV (i.e., $r_{DI} < r < r_w$)	86
3.4.	Boundary Conditions	87
3.5.	Dispersion Relationship	88
3.5.1	For Region- III and IV	88
3.5.2	For Region –II and III	90
3.5.3	For Region –I and II	91
3.6	Temporal Growth rate	93

3.7	Results and Discussion	94
3.8	Conclusion	96
CHAPTER 4	DESIGN, ANALYSIS AND SIMULATION STUDY OF DIELECTRIC FILLED S- BAND TAPERED MAGNETICALLY INSULATED LINE OSCILLATOR (MILO)	98-117
4.1.	Outline	99
4.2.	Introduction	99
4.3.	Analysis	102
4.4.	Device Modelling	106
4.5	Results and Discussion	107
	4.5.1 Cathode Misalignment Effect	113
4.6.	Conclusion	116
CHAPTER 5	SUMMARY, CONCLUSION AND FUTURE SCOPE	118-123
5.1.	Introduction	119
5.2.	Summary and Conclusion	120
	5.2.1 Chapter 1	120
	5.2.2 Chapter 2	120
	5.2.3 Chapter 3	121
	5.2.4 Chapter 4	121

5.3	Limitation of Present Work and Scope for Further Studies	122
	<i>References</i>	124-131
	<i>Author's Relevant Publications</i>	132

LIST OF FIGURES

Figure 1.1:	HPM application domain at various frequencies and power levels [Benford <i>et al.</i> (2007)].	5
Figure 1.2:	Block diagram of an HPM system [Benford <i>et al.</i> (2007)].	7
Figure 1.3:	Schematic of a Relativistic Klystron Amplifier [Barker and Schamiloglu (2001)].	10
Figure 1.4:	Schematic diagram of RBWO (a) with resonant reflector [Guinn <i>et al.</i> (1998)], and (b) with electron collector [Chen <i>et al.</i> (2002)].	12
Figure 1.5:	Schematic diagram of VIRCATOR [Barker and Schamiloglu (2001)].	13
Figure 1.6:	Schematic diagram of a Reltron [Mahto and Jain (2016)].	14
Figure 1.7:	Arletron (a) experimental set-up, and (b) MAGIC 3D simulation. [Gardelle <i>et al.</i> (2010)].	16
Figure 1.8:	All types of Gyro-devices [Gold and Nusinovich (1982)].	17
Figure 1.9:	Schematic diagram of (a) rippled waveguide SWS PASOTRON, (b) helix PASOTRON HPM source [Goebel <i>et al.</i> (1996)].	18
Figure 1.10:	Schematic diagram of (a) radial acceleratron [Arman (1996)], and (b) low impedance TTO (LITTO) [Cao <i>et al.</i> (2009)].	19

Figure 1.11:	SCO (a) fundamental mode, and (b) schematic of experiment [Marder et al. (1992)].	21
Figure 1.12:	The typical schematic view of relativistic Magnetron [Bekefi <i>et al.</i> (1976)].	23
Figure 1.13:	The typical schematic view of a Load-Limited magnetically insulated line oscillator (MILO).	25
Figure 1.14:	Process of electron emission from a velvet surface: (a) The application of the intense electric field causes the partial destruction of fiber and the creation of a dense plasma column (b) Electrons are emitted out of plasma and form a space charge current of the Child-Langmuir type. (c) Heating occurs in fiber due to the Joules effect. (d) Expansion of the plasma column at the thermal speed, and (e) Reduction of inter-electrode space by the total expansion of the plasma of the cathode [Miller (1998)].	26
Figure 1.15:	Flow chart of working mechanism of MILO	31
Figure 1.16:	Different MILO configuration [Clark <i>et al.</i> (1988)].	34
Figure 1.17:	Configuration of Hard-tube MILO (HTMILO) [Haworth <i>et al.</i> (1998)].	36
Figure 1.18:	The configuration of tapered MILO [Eastwood <i>et al.</i> (1998)].	37
Figure 1.19:	The configuration of MILO-VCO [Fan <i>et al.</i> (2007)].	38
Figure 1.20:	The illustrative image of the dual-frequency MILO [Ju <i>et al.</i> (2009)].	39
Figure 1.21:	Bi-frequency MILO configuration: (a) axial view, and (b) front view.	40
Figure 1.22:	Illustrative figure of an azimuthally partitioned axially periodic metal disk-loaded coaxial structure. (a) Sectional view. (b) Front view.	41
Figure 2.1:	Schematic of dielectric-filled periodic disc loaded Co-axial structure (a) and (b) it's unit cell.	53
Figure 2.2:	Dispersion characteristics of the partially dielectric-filled axially periodic disk-loaded co-axial SWS with structural parameter with $r_c = 29$ mm, $r_d = 43$ mm, $r_w = 87$ mm, $L = 20$ mm, and $T = 3$ mm. (a) Comparison between numerically obtained and simulation	65

	obtained dispersion characteristics. (b) Different azimuthally symmetric TM modes.	
Figure 2.3:	Comparison between interaction impedance obtained through numerical analysis and simulation.	66
Figure 2.4:	Flowchart for calculating interaction impedance using EM simulation tool “CST.”	68
Figure 2.5:	Dispersion relation for the dielectric-filled axially periodic disc loaded coaxial waveguide structure with $0 < z < L - T$ mm, $r_c = 29$ mm, $r_d = 43$ mm, $r_w = 87$ mm, $L = 20$ mm, and $T = 3$ mm.	70
Figure 2.6:	(a) Normalized phase velocity vs frequency, (b) Normalized phase velocity vs phase difference between consecutive cavities.	71
Figure 2.7:	Parametric effect on dispersion relation: (a) effect of r_c (b) effect of r_d (c) effect of r_w (d) effect of L	72
Figure 2.8:	Effect of structure design parameters on interaction impedance: (a) effect of cathode radius r_c (b) effect of a disc inner radius r_d .	73
Figure 3.1:	Schematic of a partially dielectric filled axially periodic metal disc loaded coaxial structure with beam-present in red colour: (a) sectional view, (b) unit cell (c) front view.	80
Figure 3.2:	Dispersion curve for azimuthally symmetric axially periodic metal disc loaded coaxial partially filled dielectric structure in presence of beam at voltage $V=420$ kV, current $I_a=38$ kA, (with, $r_c=29$ mm, $r_d=43$ mm, $r_w=87$ mm, $L=20$ mm and $T=3$ mm).	95
Figure 3.3:	Temporal growth rate (f_i) at different phase ($\beta_0 * L$) in radian for two conditions supported by the structure (i.e. in presence of dielectric and without dielectric).	96
Figure 4.1:	Schematic diagram of dielectric filled tapered MILO.	102
Figure 4.2:	Single dielectric filled cavity and its equivalent parallel circuit of resonance system.	103
Figure 4.3:	Schematic and its equivalent circuit of tapered SWS cavity with partially filled with low loss dielectric material.	104
Figure 4.4:	Magnetic field contour plot of the SWS structure in π -mode oscillation at 2.6775 GHz.	107
Figure 4.5:	Dispersion relation of tapered slow wave structure with and without dielectric filling inside cavities.	109

Figure 4.6:	Temporal RF output peak power obtained at the output port of the device without dielectric loading inside the cavities.	109
Figure 4.7:	FFT of RF signal obtained at output port without dielectric loading inside the cavities.	110
Figure 4.8:	Temporal RF output peak power obtained at the output port of the device with dielectric ($\epsilon_r=4$) loading inside the cavities.	110
Figure 4.9:	FFT of RF signal obtained at output port with dielectric ($\epsilon_r=4$) loading inside the cavities.	108
Figure 4.10:	Different modes excited inside the device due to cathode misalignment, (a) degenerative TE_{11} mode (b) desired TM_{01} mode.	114
Figure 4.11:	Temporal RF output peak power obtained at the output port of the device with dielectric ($\epsilon_r=4$) loading inside the cavities and cathode axis misalignment with 5%.	114
Figure 4.12:	FFT of RF signal obtained at output port with dielectric ($\epsilon_r=4$) loading inside the cavities after $\sim 5\%$ cathode misalignment.	115

LIST OF TABLES

Table 1.1:	HPM device application in several domains.	6
Table 1.2:	Comparison of MILO with other HPM Sources.	24
Table 1.3:	Chronological order of development of MILO device.	32
Table 4.1:	Device design specifications for dielectric filled tapered MILO	106
Table 4.2:	Comparison of device RF performance with published and present simulation of the tapered MILO.	116

LIST OF ABBREVIATIONS

Abbreviation	Full form
HPM	High power microwaves
RF	Radio Frequency
PRF	pulse repetition frequency
DEW	Direct energy weaponry
EM	Electromagnetic
TWT	Traveling wave tube
RBWO	Relativistic backward wave oscillator
MILO	Magnetically insulated line oscillator
GHz	Giga-hertz
MHz	Mega-hertz
GW	Giga-watt
MW	Mega-watt
Ns	Nano-second
RKO	Relativistic klystron oscillator
RKA	Relativistic klystron amplifier
VIRCATOR	Virtual Cathode Oscillator
PASOTRON	Plasma Assisted Slow- Wave Oscillator
TTO	Transit-Time Oscillator
SCO	Split Cavity Oscillator
CRM	Cyclotron resonance masers
FEL	Free Electron Laser
SWS	Slow-wave structure

TM	Transverse Magnetic
TE	Transverse Electric
EEE	Explosive electron emission
CTL	Coaxial transmission line
UHF	Ultrahigh frequency
RBF	Relativistic Brillouin flow
VCO	Virtual cathode oscillator
PIC	Particle-in-cell
HEM	Hybrid electromagnetic
HE	Hybrid electric
FFT	Fast Fourier Transform
AC	Alternating Current
DC	Direct Current
TTO	Transit time oscillator
DFMILO	Dielectric filled magnetically insulated line oscillator
TGR	Temporal growth rate
SCW	Space charge wave
cm	Centimeter
mm	Millimeter
kV	Kilo-volt
kA	Kilo-ampere
TEM	Transverse Electromagnetic

LIST OF SYMBOLS

Symbol	Details
v_e	Electron velocity
v_p	phase velocity
L	Equivalent inductance for single cavity resonator
C	Equivalent capacitance for single cavity resonator
$C_{i,z}$	Coupling capacitance
C_{eq}	Equivalent capacitance of parallel resonator circuit
r_c	Cathode radius
r_d	Disc inner radius
r_w	Outer wall radius
L	Periodicity
T	Thickness
R_{ai}	Disc inner radius with different depth
g	The gap between disc inner radius and cathode
E	Electric field
H	Magnetic field
β_n	Axial propagation constant
ω	Angular frequency
γ_n	Radial propagation constant
k	Free space propagation constant
J_0	Bessel functions of 1 st kind with zero order
Y_0	Bessel functions of 2 nd kind with zero order
c	Speed of light
F	Frequency

A_z	Vector potential
μ	Permeability
ε	Permittivity
I_θ	Azimuthal current
Z_0	Characteristic impedance
ζ_n	velocity shifted frequency
Γ_n^*	Radial beam parameter in presence of beam
ω_p	Plasma frequency
P	Total transmitted RF power
K	Interaction Impedance
l_{stub}	Length of stub
λ	Wavelength
λ_g	Guided wavelength
l_T	Length of tapered cathode
\hat{v}_z	Axial drift velocity
γ	Relativistic factor
P_z	Axial momentum
n_e	Charge number density
r_e	Electron beam radius
η	Normalized factor
$\delta(r - r_e)$	Delta function
I_A	Alfven current
γ_n^*	Radial propagation constant in presence of electron beam
v_{slow_sc}	Slow space charge velocity
f_i	Imaginary value of frequency
f_r	Real value of frequency
I_a	Anode current
I_{cr}	Critical current

B_c	Cut-off magnetic field
V_H	Hull cut-off voltage
V_{BH}	Buneman-Hartee voltage
E	Electron charge
m_0	Electron mass
χ_{np}	Modal root of the nth order Bessel–Neumann combination
dB	Decibel
MW	Mega-watt

PREFACE

Due to its numerous commercial and military uses, high-power microwave (HPM) has gained immense popularity in the microwave world. Researchers and academics from all over the world are interested in R&D in this field due to the creation of RF in millimeter-wave ranges and the dual-frequency generation using a single HPM device. A HPM source is a device that has a frequency range of 1–300 GHz and can generate RF power more than 100 MW. The major application fields for HPM include indirect energy weapons, communication, radar, UWB, power beaming, linear colliders, and (DEW). Different sub-systems are utilised throughout the whole process of HPM generation and application, starting with the prime power supply and following on through pulsed DC power formation, a microwave source, a mode converter, and an antenna. Each of these several HPM subsystems has a distinct function in the generation and application of RF energy. The primary component of the entire microwave generation process is the microwave or HPM source. A relativistic magnetron, a relativistic klystron, a relativistic backward wave oscillator, a relativistic gyrotron device, a vircator, a reltron, and a magnetically insulated line oscillator are examples of HPM sources that can produce RF power (MILO). Cherenkov radiation, transition radiation, and Bremsstrahlung radiation are the three basic categories used to describe the various radiation processes used by these HPM sources. The HPM source MILO, which employs the Cherenkov radiation process, is the basic foundation of this research. When compared to other HPM sources, the MILO requires no external magnetic field, which makes it compact, lightweight, and suitable for usage on many mobile platforms.

Similar in operation and theory to a linear magnetron, MILO is a crossed-field high power microwave device. Slow-wave tubes and magnetically insulated electron flow technology are

combined to make it operate. Two DC power sources are used in a microwave oscillator, which needs an external DC magnetic field, in order to demonstrate magnetic insulation and cause electrical breakdown when higher voltages are approached. Because of their extremely high inherent impedance, these oscillators can only function at very low power levels. Therefore, an oscillator that can function at the lower impedance and solve the voltage matching issue would be appropriate for effective operation at greater power levels. In order to solve the aforementioned issues, MILO has been employed, where the necessary magnetic field is generated by the electron-beam current itself, rather than by a separate magnet, making the device more compact and lightweight. The design of MILO must be improved in order to prevent some serious problems, such as the issue of pulse shortening, asymmetric mode generation and mode competition, shot-to-shot reproducibility, the requirement of high pulse rate frequency, and long cathode life, which are still observed as challenges for device development. The Electromagnetic analysis of partially dielectric filled in SWS of MILO by the use of field matching approach in beam absent case, and also the effect of dielectric material on device parameter are the prime concern for this thesis. Further the electromagnetic analysis of beam wave interaction in partially dielectric filled MILO has been done in this research. The partially dielectric filled MILO was simulated by the CST studio suite and cathode misalignment effect was also analyzed in this thesis.

The author has periodically published parts of the current work in reputed publications, including IEEE Transaction on Plasma Science.

If it proves helpful in the design of partially dielectric filled MILO, the author will consider his little effort a success.